Results of the *Telstar* Satellite Space Experiments

By P. T. HUTCHISON and R. A. SWIFT

(Manuscript received March 1, 1963)

This paper describes how the Telstar satellite has performed in space. Included is information on changes in the temperature, spin rate, spin-axis precession, orbital parameters and power levels of the satellite signals, and comments on the behavior of the electrical circuits in the space environment.

I. INTRODUCTION

This paper describes the initial performance and changes in the electrical characteristics of the communications repeater, command system, and telemetry system and changes in the temperatures, spin rate, spin-axis precession, and other physical phenomena occurring in the Telstar spacecraft during the first months of operation.

One of the objectives of the Telstar experiment was to obtain information on the performance of an active communications satellite repeater over an extended time interval and to obtain data that would be applicable in the design of a commercial communications satellite. To this end, the Telstar spacecraft has been closely monitored since it was launched. The satellite is monitored by measurements of signals received at the ground stations and by telemetry. Observations at ground stations give orbital, satellite-orientation, antenna-pattern, and signal-level data. Telemetry gives satellite orientation, solar plant output, satellite temperature, and electrical performance data.

The spacecraft was spin-stabilized and injected into orbit with its spin axis nearly perpendicular to the ecliptic plane. This insured the most favorable coverage of the earth by the Telstar antennas, the maximum output power of its solar cells, and the most favorable skin temperature distribution. The value of the spacecraft as a communications satellite is a function of how well it retains this orientation as it orbits the earth. Measurements of the changes in this orientation indicate an average precessional torque of 3×10^{-6} pound foot due to the residual

magnetic moment of the satellite. This type of information is helpful in developing orientation schemes for future satellites.

The spacecraft was designed and tested to withstand the environmental conditions it would see throughout launch and its life in orbit, based on the known and assumed aspects of its environment. By placing the spacecraft in orbit, the assumptions made could be evaluated.

The most meaningful test of a communications satellite is the test of how well its electronics circuitry operates under actual space conditions. The results of the successful communications experiments are discussed in a separate paper[1] in this issue. In this paper, the emphasis is placed on changes that may have occurred since launch on July 10, 1962.

When the Telstar satellite was launched, it was injected in the predicted orbit with the spin axis favorably orientated with respect to the sun at a time of day which resulted in 14 full sunlit days before the satellite entered periods of eclipse. The initial orbit parameters were as follows:

Apogee	3047 nautical miles
Perigee	515 nautical miles
Inclination	44.79 degrees
Spin rate	177.7 rpm
Solar aspect	90.5 degrees

During the period from launch on July 10, 1962, to the time of interruption of the VHF command system on November 23, 1962, there were only minor variations in the power levels and the operating characteristics of the communications repeater in the satellite. The satellite temperature, attitude, visibility times, and eclipse times have varied as anticipated. It is the purpose of this paper to discuss qualitatively the causes and effects of the expected and unexpected variations in satellite performance.

II. SOLAR ASPECT

Solar aspect is defined as the angle between the sun-satellite line and the satellite spin axis, measured from the telemetry antenna. This angle is determined by sampling the currents from (each of) six solar cells mounted at the ends of three mutually perpendicular axes on the satellite skin. The output currents of the six cells, together with their known geometric arrangements, uniquely define the solar aspect angle[2] with an accuracy of $\pm 0.5°$. The curve shown in Fig. 1 indicates the spacecraft orientation for the twelve-week period following launch.

The reasons for the shape of this curve are twofold. First, the satellite spin axis at injection was not quite normal to the plane of the ecliptic.

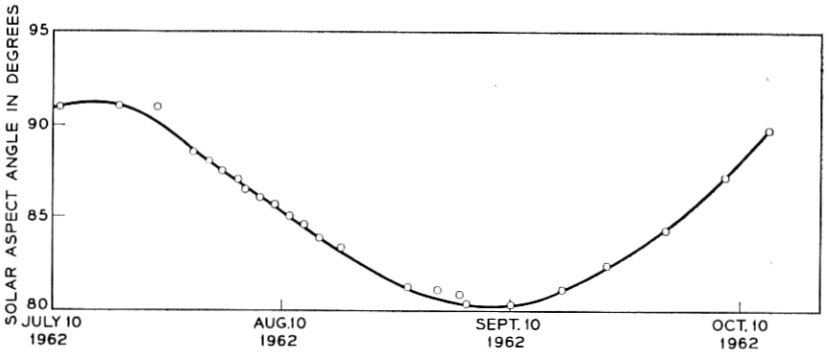

Fig. 1 — Telstar spacecraft — solar aspect angle versus time.

As both the earth and the orbit rotate with respect to the sun, the spin-axis projection alternately decreases and increases. Second, the attitude of the spin axis in inertial space is varying due to a precessional torque. This will be discussed later. The main effects of solar aspect deviations from 90° on the satellite's performance are to reduce the available power from the solar cells and to change the skin temperature distribution. This occurs because the solar-cell distribution is not isotropic over the satellite surface; however, the small deviations noted to date have not resulted in a significant change in output from the power supply.

III. ATTITUDE

Changes in the solar aspect angle are due in part to attitude changes in inertial space. Attitude is expressed in the spatial coordinates of declination and right ascension. In terms of an infinite sphere with the earth's lines of latitude and longitude projected upon it, declination corresponds to the latitude and right ascension to the longitude measured eastward from the vernal equinox. The coordinates of the attitude indicate the intersection of a line coinciding with the spin axis that starts at the center of the satellite and goes through the telemetry antenna and the infinite sphere.

The analysis of three sets of data serves to determine the attitude of the satellite. As previously mentioned, solar sensors indicate the angle between the satellite spin axis and the sun. Another angle is obtained from a series of light flashes observed from mirrors mounted on the satellite.[3] The time of the flash occurrence yields an indication of the angle between the spin axis and the satellite-ground station line, sometimes denoted as the earth aspect angle of the satellite. These two angles form tangent cones with a common apex. The intersection is a straight

line whose direction is determined from the knowledge of initial launch conditions. Fig. 2 is a plot of satellite attitude during the first three months, equivalent to approximately 800 orbits.

Changes in satellite attitude are caused by a torque generated by the interaction of the satellite magnetic moment and the earth's magnetic field. Prior to launch, a compensating magnet was mounted on the satellite to reduce the effect of the TWT magnetic field. However, a residual moment causing torques on the order of 10^{-6} pound feet remained. Owing to the nodal regression of the Telstar satellite orbit, the precessional torque rotates with respect to the satellite. The torque induces a continuously changing attitude of the satellite moment of momentum and a rapid precession about the momentum vector. Precession dampers within the satellite effectively eliminate this rapid precessional motion. As seen in Fig. 2, attitude changes increase from orbit to orbit as the satellite spin decreases; that is, the satellite tendency to rotate due to torques increases with spin decay.

The satellite is equipped with a coil of wire around its equator and a direct-current supply which, when activated, either reinforces or reverses the axial magnetic moment, thereby providing a means for attitude correction.

IV. SPIN RATE

The effect of the precessional torque is heightened by the steady decrease in the satellite spin rate. The major retarding torque causing this

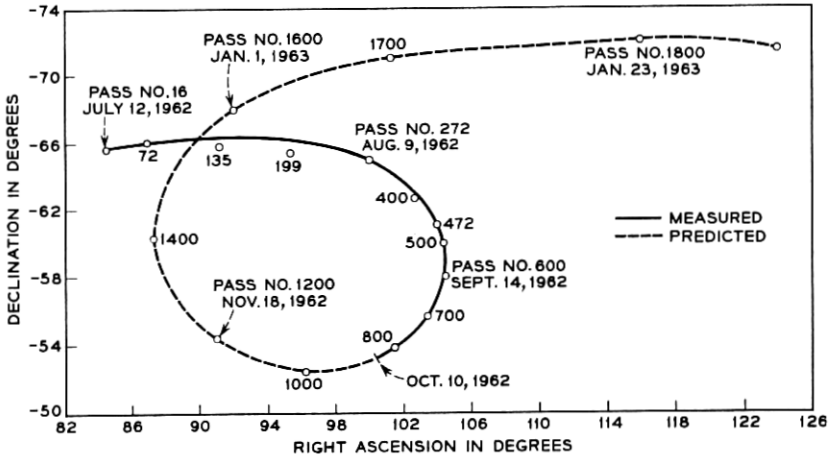

Fig. 2 — Telstar satellite attitude.

spin decay is produced by eddy currents generated in the satellite as it rotates in the earth's magnetic field. Since the instantaneous torque is dependent on the spin rate, the satellite would undergo a pure exponential decay if it were rotating in a uniform field. However, the effective magnetic vector, which is the component normal to the spin axis, is a function of both satellite attitude and altitude, geomagnetic field along the orbit, the regression of the orbit plane, and the advance of perigee. Satellite attitude and nodal regression are considered to be secondary effects. Fig. 3 is a sketch of field variation and satellite latitude versus orbital period. The dashed line indicates the satellite latitude. Shortly after injection, the perigee occurred near the equator. As the orbit precessed, the perigee moved toward the region of higher field strength. The net effect is to continuously alter the slope of the exponential decay curve, resulting in an initial decay that was almost linear, as shown in Fig. 4.

On the basis of this curve, it is calculated that the spin rate will be

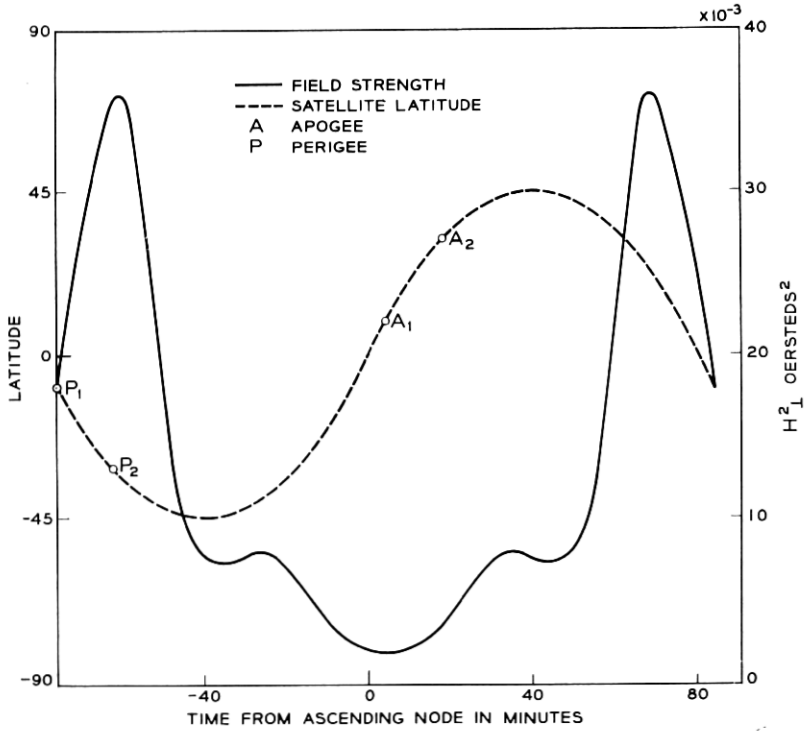

Fig. 3 — Field strength and satellite latitude versus time from ascending node.

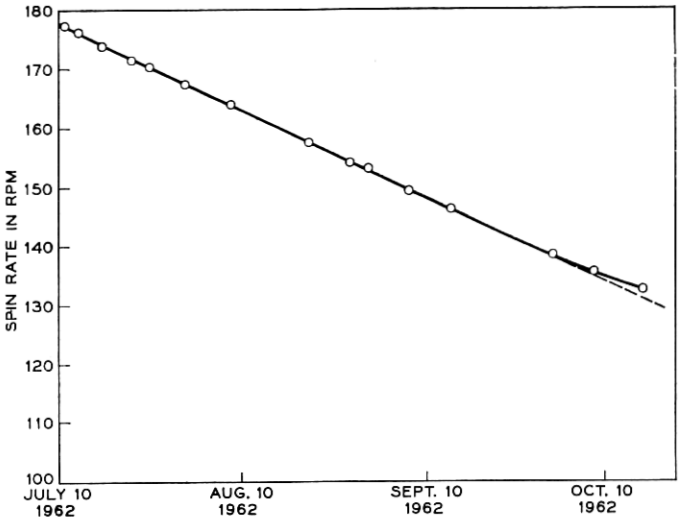

Fig. 4 — Telstar satellite — spin rate versus time.

reduced from an initial rate of 177.7 rpm to 66 rpm in about 330 days,[4] and the spin rate will therefore stabilize the Telstar satellite for about two years.

V. VISIBILITY TIME

It has been shown that the motion of the perigee within the orbit plane affects the satellite spin rate and attitude. Owing to the ellipticity of the orbit, the perigee motion also affects the minimum usable time per day. Usable time is defined as the time the satellite remains at least 7.5° above the horizon. The higher the satellite is during a pass, the longer it will be visible to a particular ground station. As the perigee moves to its most southern latitude (−45°), the apogee is almost over the Maine ground station; and as shown in Fig. 5, the usable time reaches a maximum. Maximum visibility occurs when apogee is over the ground station for two reasons. This is the time when the greatest portion of the orbit is visible and also the time in orbit when the satellite velocity is a minimum.

VI. ECLIPSE DURATION

Satellite eclipse duration is important insofar as it affects the satellite temperatures and the ability of the solar cells to recharge the batteries. A curve of satellite eclipse time per orbit is shown in Fig. 6.

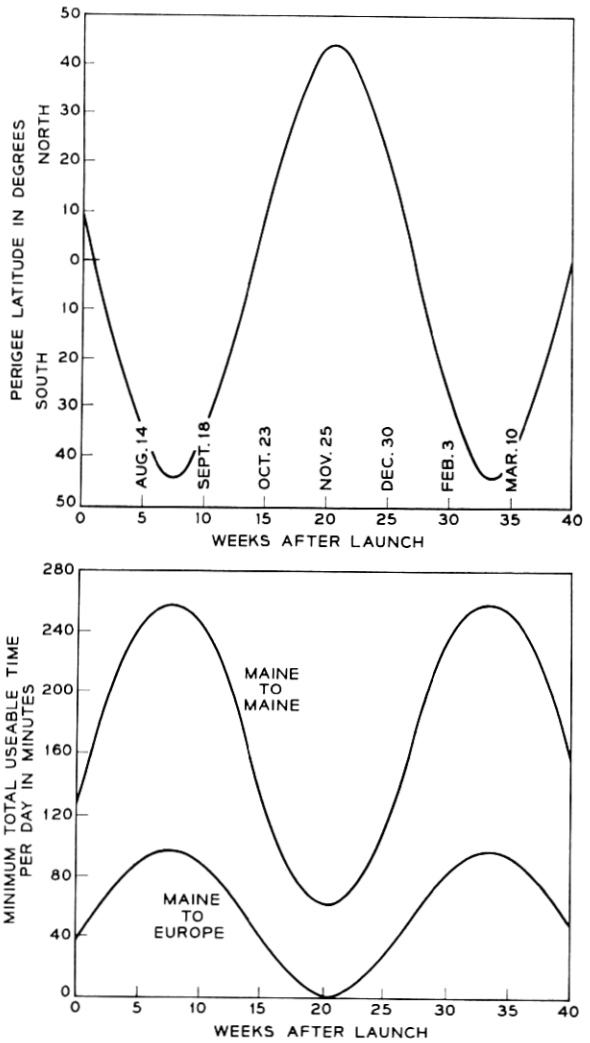

Fig. 5 — Telstar satellite — perigee latitude and minimum usable time per day.

Between July 21, 1962, and January 8, 1963, the satellite was to be in shadow for a period of about 30 minutes per orbit on the average. The shape of this curve is principally a result of three motions·

(1) The motion of the earth and the orbital plane about the sun.

(2) The regression of the orbital plane.

(3) The advance of the apogee and perigee within the orbital plane.

The effect of these motions on the orbit-earth-sun orientation is shown

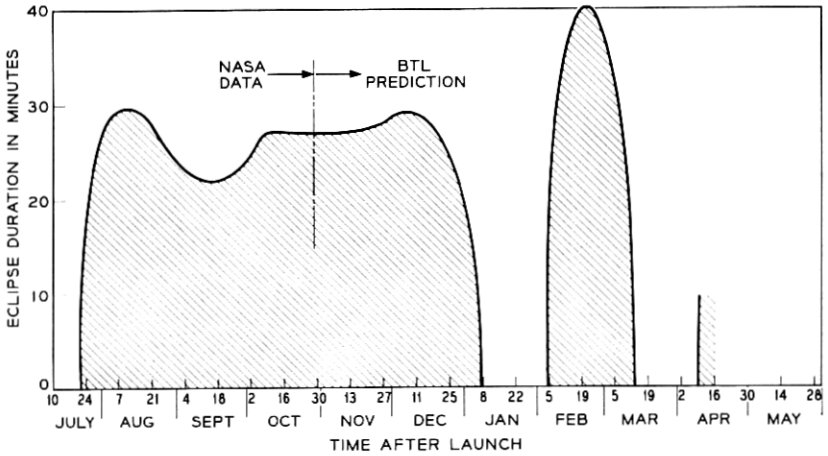

Fig. 6 — Predicted satellite eclipse duration.

pictorially in Fig. 7. It is seen that the orbit rotates clockwise in the direction opposite to the earth's spin as the earth moves counterclockwise about the sun. The perigee moves in the direction of the satellite motion within the plane of the orbit. The perturbing influence causing these motions is due principally to the attractive forces associated with the earth's equatorial bulge.

Shortly after the Telstar satellite first went into eclipse, July 21, 1962, the perigee was in shadow. Each day the satellite goes into eclipse approximately two minutes later than on the previous day. This is shown in Fig. 8, where eclipse occurrence time after ascending mode is plotted against calendar time and orbit number. The vertical height of the gray area on any particular day represents the eclipse time. This curve was made for passes occurring near midnight EDT.

VII. SATELLITE TEMPERATURES

The satellite temperatures of major interest are those of the electronics canister and the solar cells. The energy transfer paths determining these temperatures are shown schematically in Fig. 9.

It is important that the solar-cell temperatures be kept low for two reasons: first, the conversion efficiency of the solar cell plant decreases with increasing temperature; second, the solar cell life decreases with sustained high temperatures. Temperatures within the canister must be kept within certain ranges to ensure optimum system operation.* It will

* In the satellite, the nickel-cadmium battery is the component most sensitive to temperature variations.

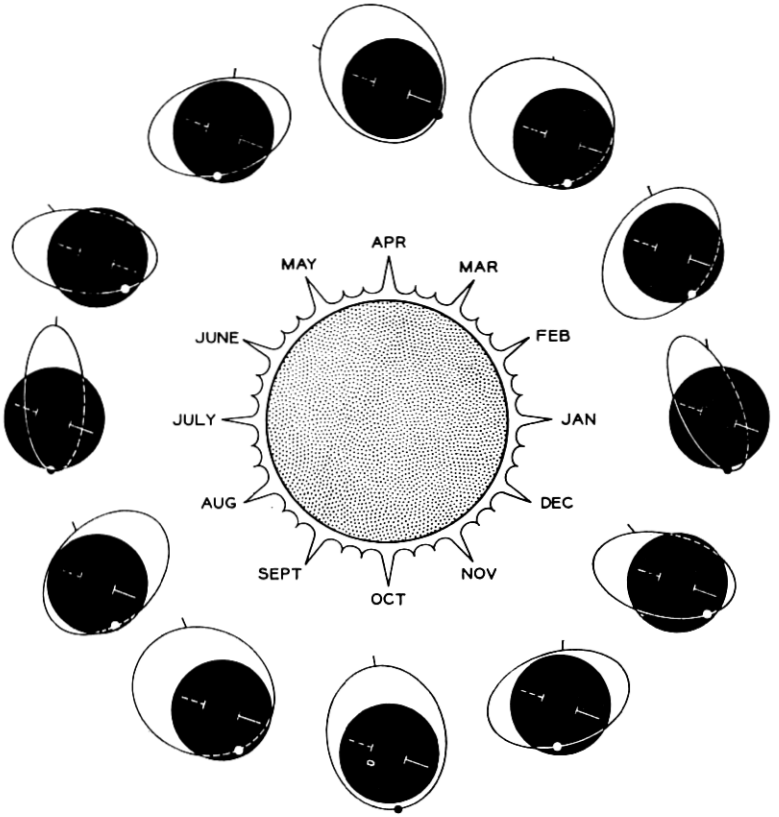

Fig. 7 — Orbital motion of spacecraft.

be seen in the following how solar aspect, in addition to periods of eclipse, influences satellite temperatures and power-plant efficiency.

The Telstar spacecraft geometry and the near isotropic distribution of solar cells makes the total energy absorbed nearly insensitive to the satellite orientation or attitude. Therefore, the mean radiant temperature, T,* depends chiefly on the energy incident on the satellite and the

* The mean radiant temperature, T, is determined by equating the incident energy to the radiated energy.

$$\text{heat in} = \text{heat out}$$

$$\pi R^2 \alpha (S + A + I) = 4\pi R^2 \epsilon \sigma T^4$$

$$T^4 = \frac{1}{4} \frac{\alpha}{\epsilon} \frac{1}{\sigma} (S + A + I)$$

where

α = absorptivity
ϵ = emissivity
σ = Stefan Boltzmann constant
R = radius.

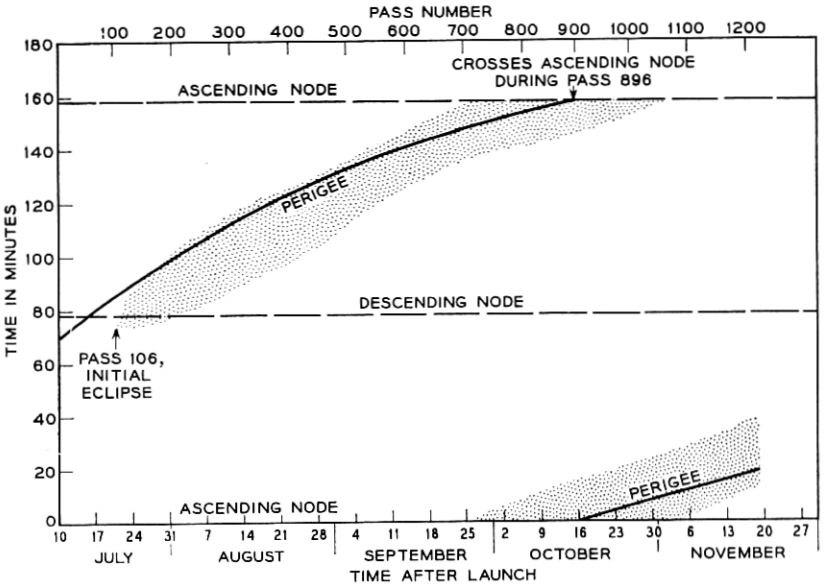

Fig. 8 — Telstar spacecraft orbital events.

satellite's surface characteristics. Both the skin temperature distribution and the temperatures within the electronics canister are related to the mean radiant temperature and the energy dissipated within the chassis, Q. However, the nature of the skin temperature distribution affects the solar plant; large temperature extremes over the satellite surface result in lower net power.

Since the spacecraft is spinning, the most favorable skin temperature distribution occurs when the sun rays are normal to the spin axis.

7.1 *Satellite Skin Temperatures versus Time*

Typical satellite skin temperatures for the first three months after launch are plotted in Fig. 10. During this period the solar aspect has varied over a range of 10°. The effect of the changing aspect has been to increase the temperature of the pole inclined toward the sun. The period of temperature variation closely corresponds to that of the variation in solar aspect. The difference is accounted for by the effects of secondary radiation, infrared energy radiated from the earth, and solar energy reflected from the earth. These data were recorded when the satellite was well out of eclipse. It is evident that the average of these skin tempera-

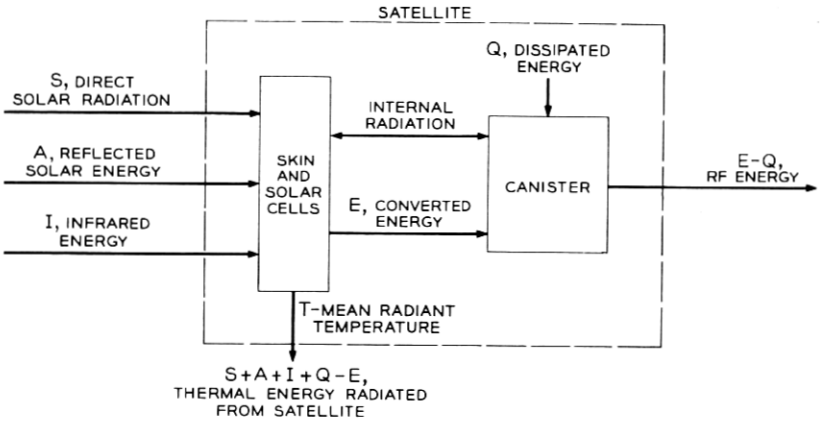

Fig. 9 — Spacecraft energy transfer.

tures has decreased, even though the solar flux density is increasing as the earth moves closer to the sun. This indicates that the effect of eclipse is greater than the effect of the increasing solar flux density.

7.1.1 *Skin Temperatures During a Typical Orbit*

Fig. 11 indicates how the skin temperatures vary as a function of time from perigee. These data were recorded August 16, 1962, and are repre-

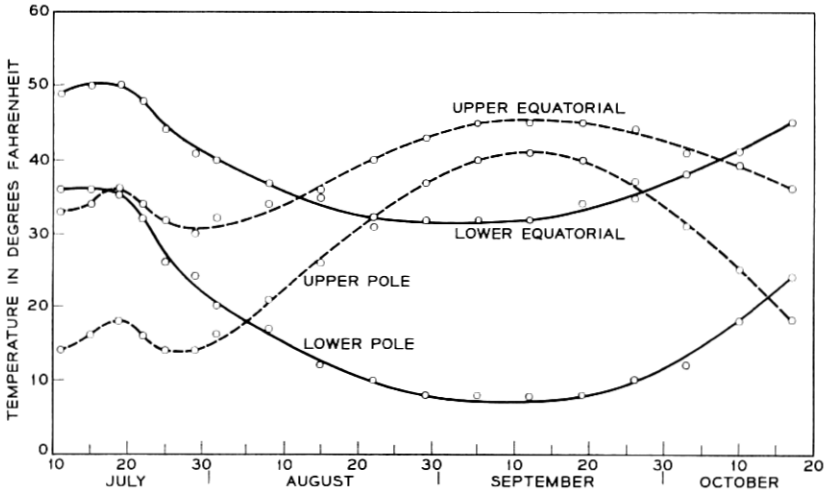

Fig. 10 — Skin temperature versus time.

sentative of a few orbits on that day. The effect of solar aspect is clearly seen during the period 60 minutes to 130 minutes. After 130 minutes the satellite went into eclipse. During eclipse the upper pole temperature was lower than the lower pole temperature. This temperature difference is a result of energy reflected and energy radiated from the earth. While in eclipse, the lower hemisphere was favorably inclined with respect to the earth for heat transfer from these secondary sources.

7.1.2 *Skin Temperatures During Eclipse*

The Telstar satellite first went into eclipse on July 21, 1962, and by August 16, 1962, the perigee was in shadow for 30 minutes. As shown in

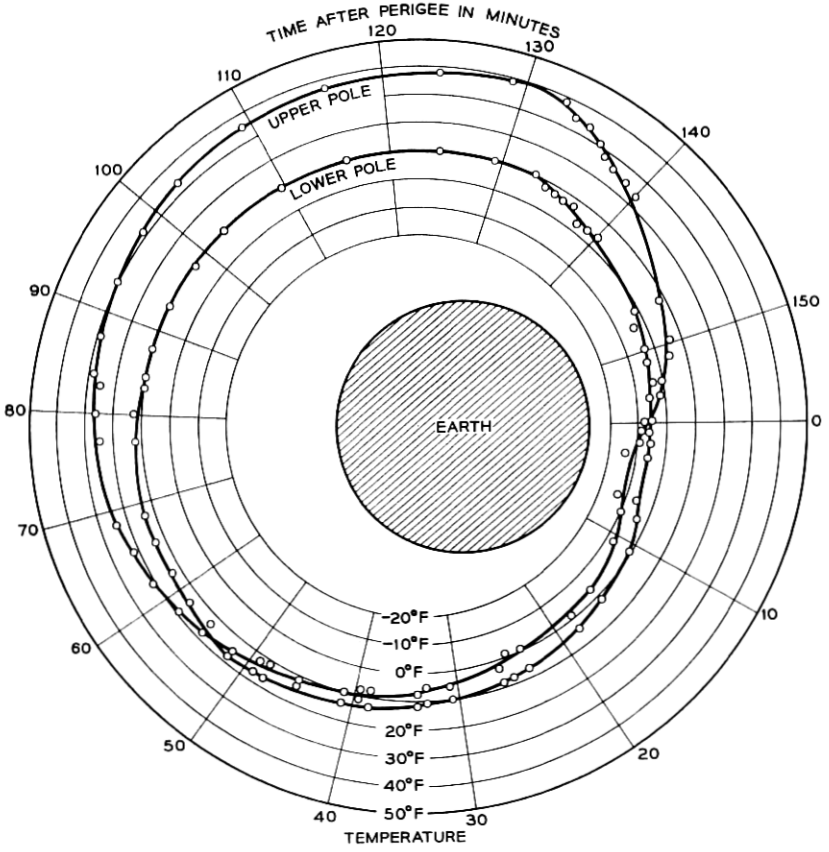

Fig. 11 — Skin temperature versus orbital position.

Fig. 12, the skin temperatures dropped sharply as the satellite went into eclipse, but were slow to return as the satellite emerged from shadow. This is best explained in terms of the skin surface properties. Since the average value of the absorptivity to emissivity ratio, α/ϵ, is about 0.65, the spacecraft emits energy faster than it will absorb.

7.1.3 *Skin Temperatures During Launch*

The satellite was designed to operate satisfactorily over wide temperature variations during both orbit and launch. During the launch

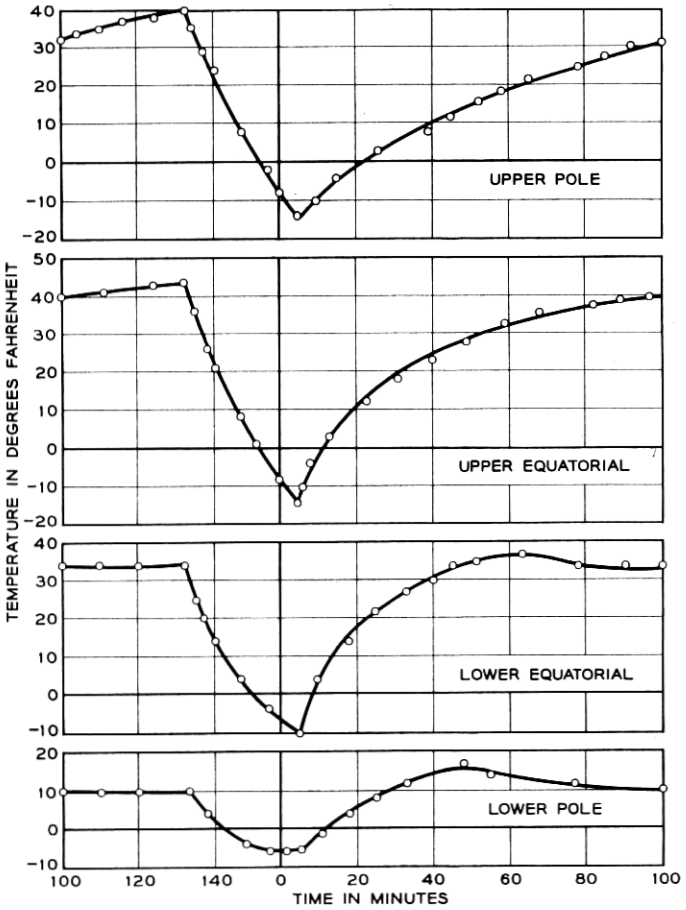

Fig. 12 — Satellite skin temperature during typical orbit with eclipse.

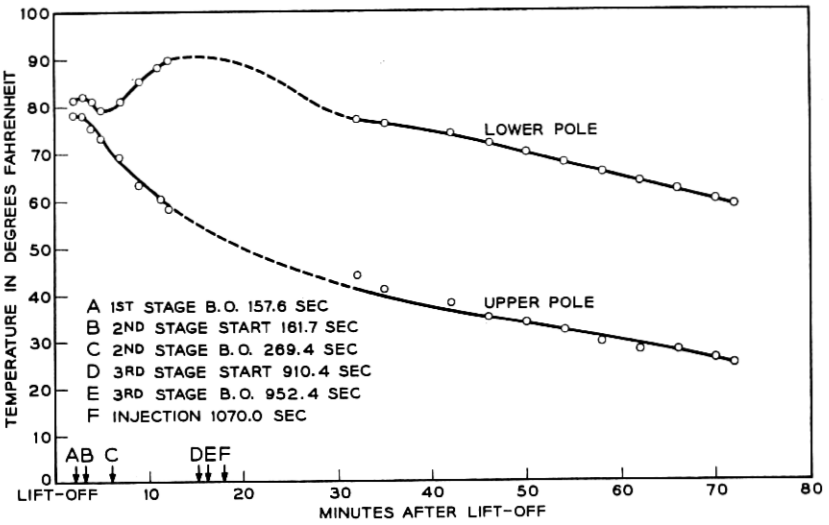

Fig. 13 — Skin temperature during launch.

phase, the satellite was protected from aerodynamic heating by a fiberglass shroud which separated from the second stage prior to third-stage ignition. As seen in Fig. 13, the shroud was effective in maintaining reasonable skin temperatures on the satellite. Initially, the lower pole temperature rose slightly; it is believed that energy conducted from the missile was responsible for this temperature increase.

7.2 *Temperatures Inside the Electronics Canister*

The electronics canister is a hermetically sealed unit which houses 95 per cent of the electronics circuitry of the satellite. The canister is completely covered with an aluminized Mylar "blanket" when the bellows-actuated shutters, which cover the upper and lower domes, are closed.[5] When the shutters are open, the emissivity of the domes is increased, so the shutters control the canister temperatures. The solar plant furnishes, when new, a power of about 14 watts continuously except when the satellite is in eclipse. This primary source of power energizes the electronics equipment, charges the battery, and heats the canister.

Telemetry information from 21 thermistors located inside the electronics canister gives the temperatures of various components and sub-

assemblies from which rough temperature gradients can be found. Nine of these sensors are located in the switching regulator, in the dc-to-dc converter, and near the collector of the traveling-wave tube (TWT). These sensors are located at expected local hot spots, so the TWT can be turned off before the temperature exceeds the safe limit at these points. The remaining 12 sensors are located on various subassemblies where the temperature affects the calibration of a telemetry channel, or near points of special interest such as the Ni-Cd cells.

The temperature of the Ni-Cd cells is important, so this temperature is one of two chosen as representative for discussion. Maximum and minimum telemetry readings of the Ni-Cd cells are plotted as a function of time in Fig. 14(a). The general wavy nature of these curves does not mean that the temperature extremes vary this much from week to week, but is a result of the fact that telemetry data are taken only during certain times in each orbit and the temperatures of all parts of the satellite are dependent on satellite position as shown in Fig. 11. Also, the variation of temperature over one day depends partially on how much the TWT is used. During the time the TWT is used, the battery is discharging, so stored energy is furnished by the battery to the tube and other circuits which convert most of the electrical energy to heat energy. After long use of the TWT, the battery is discharged, and energy from the solar plant goes into chemical energy in the battery instead of going into heat energy, as it does when the battery is fully charged. Thus, there is a short time after TWT use when there is a slight drop in battery temperature. The TWT was operated more in August than at other times because of longer visibility from Andover, Maine, during this period.

The temperature of the waveguide used as part of the up converter is plotted as a function of time in Fig. 14(b). This plot shows much less temperature variation than the plot of battery temperature because the waveguide is a good heat sink.

VIII. RADIO-FREQUENCY POWER LEVELS

In this section, telemetry readings are presented to show that there have been no appreciable changes in the power levels of the three signals radiated from the satellite, the local oscillator signals used for the modulators in the satellite, or the signals associated with the microwave carrier supply (MCS). In order to prove the invariance of some of these power levels, it is necessary to show that the characteristics of the TWT and the beat-oscillator (BO) modulator have not changed. Microwave

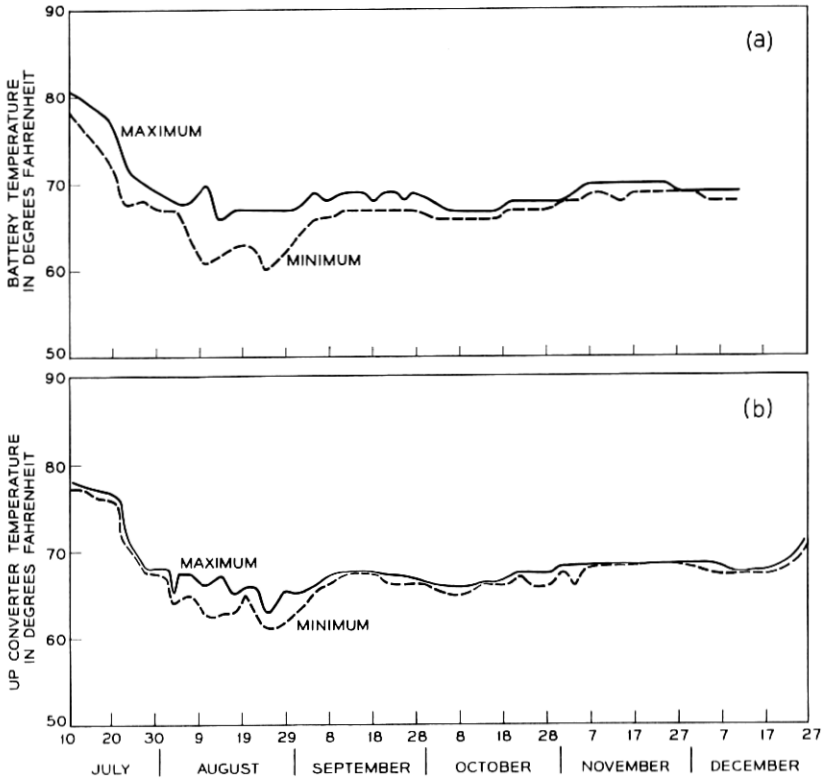

Fig. 14 — (a) Battery temperatures since launch; (b) up-converter temperature since launch.

power levels and their associated telemetry channels are shown in Fig. 15, which gives a simplified block diagram of the communications repeater. Fig. 16 is a block diagram which shows the VHF beacon and other VHF circuitry. Both figures show frequencies accurate to two decimal places, but for simplicity approximate values will be used in the discussion. Throughout this and the following sections, reference is made to Table I, which gives voltages, currents, powers, and temperatures for important telemetry channels. The purpose of these representative data is to show changes in these quantities, and not the actual values. In particular, some of the power monitors are inaccurate in determining absolute values, but changes in readings are significant. The telemetry channel numbers used in the discussion are for conven-

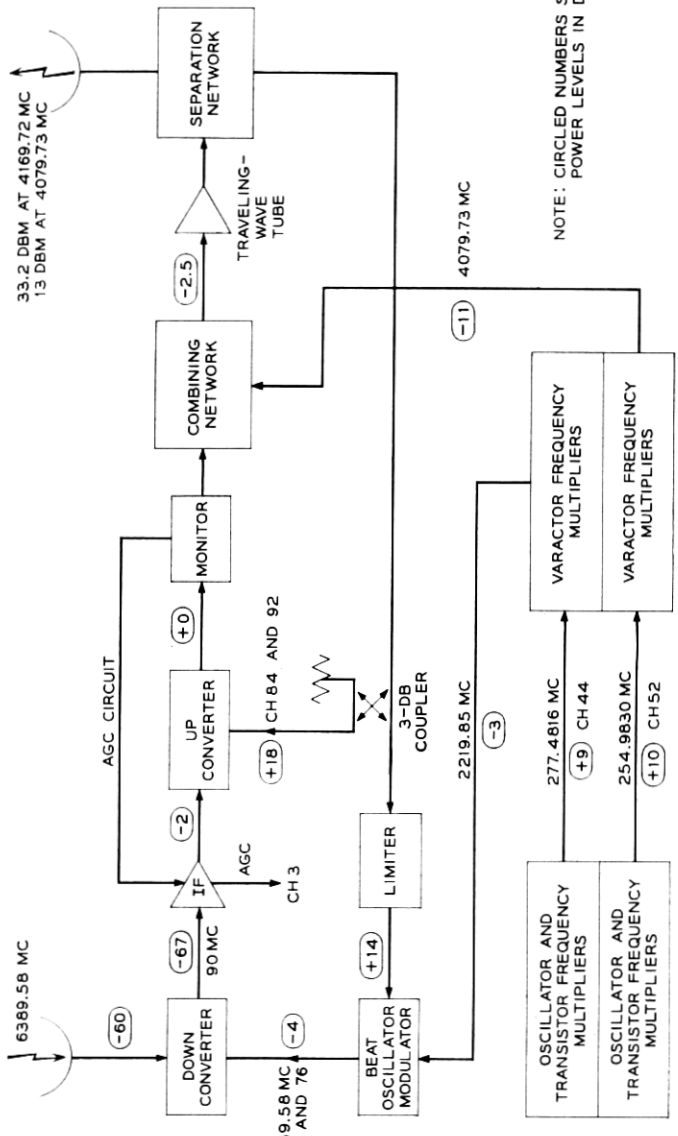

Fig. 15 — Communications repeater.

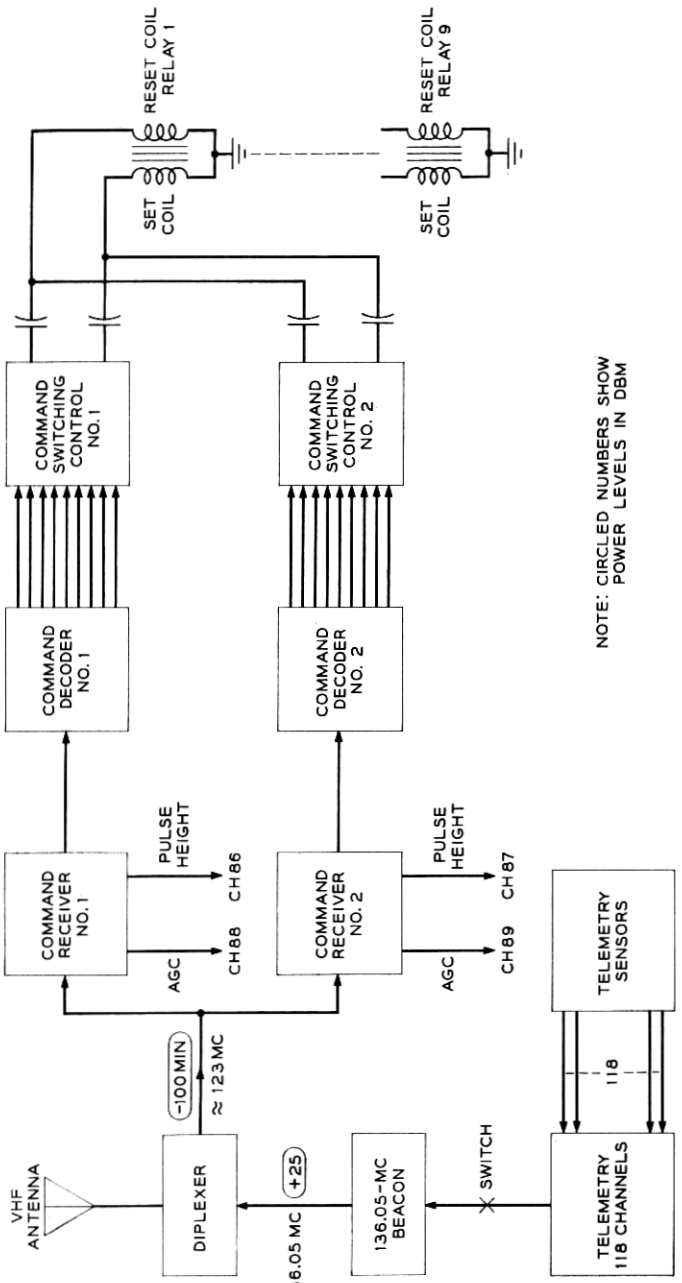

Fig. 16 — Command and telemetry systems.

ience only; the assignment of the actual channel numbers was to a large degree arbitrary.

8.1 *Microwave Beacon*

As Fig. 15 shows, the same 4080-mc frequency is used to provide the microwave beacon signal and to pump the varactor diodes in the up converter and BO modulator. The reflex circuit which provides sufficient power at this frequency is discussed by another paper[6] in this issue. Since the insertion losses of all the filters in the satellite are known, the 4080-mc power levels at any point can easily be calculated if the level at one point is known. The 4080-mc signal is used to pump the self-biased varactor diodes in the up converter, so the bias voltages on these diodes, monitored by telemetry channels 84 and 92, are used to measure the power levels at this part of the circuit. The IF signal level into the up converter is small (−2 dbm) so the bias voltages on these diodes are due almost entirely to the 18-dbm pump at 4080 mc. Figs. 17(a) and 17(b) show the relationships between the bias voltages and the pump

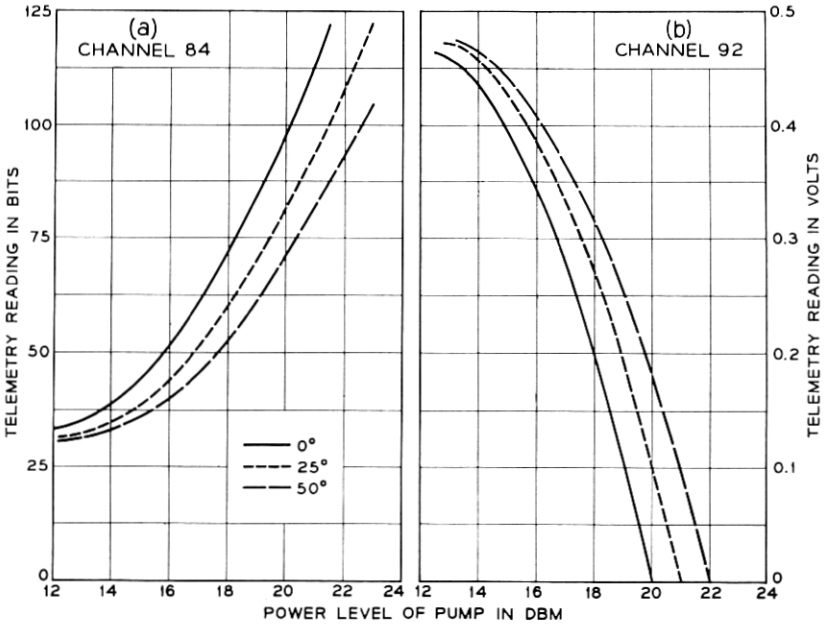

Fig. 17 — Telemetry readings versus pump level for the up converter.

input.* A normal power level of 18 dbm at the input to the up converter corresponds to a power of 18.6 dbm to the antenna feed system. Insertion loss of the antenna and feed is approximately 1.6 db, so the normal radiated microwave beacon power is 17 dbm.† The exact insertion loss of the antenna and feed system is not known over the temperature range experienced by the satellite, but the variation is known to be less than 0.1 db.

The data for channels 84 and 92 in Table I show about a ½-db disagreement in the measured pump level, but the change in power since launch, as shown by both channels, is very small. Powers are calculated to three significant figures in an effort to show changes in level, but obviously no such absolute accuracy is claimed by this method of monitoring the power.

When no power at 6390 mc is transmitted to the satellite, only noise (about −6 dbm) drives the TWT, and the power output of the tube at 4080 mc increases[6] about 2 db, as shown in Fig. 18. This results in an increase in the radiated power at 4080 mc, but this is normal circuit behavior and does not represent any change in the satellite circuitry.

8.2 *The Communications Signal*

The power output of the satellite in the 4170-mc band is not monitored, but the approximate output can be calculated by using known values of satellite antenna gain and path loss and the measured values of received signals on the ground. However, changes in the power output can be more accurately determined by another method. As Fig. 15 shows, the TWT in the satellite amplifies signals at both 4080 and 4170 mc. Because the tube is driven into partial saturation by the signal at 4170 mc (see Fig. 18), changes in the output level at this frequency are accompanied by greater changes in the level of the signal at 4080 mc. The power at 4080 mc is monitored, so changes in the power level at 4170 mc can be measured indirectly if the characteristics of the TWT do not change and if the input signal to the TWT is constant. The drive to the TWT is constant when the signal at 6390 mc is within the AGC range. The data in Table I show that the helix and accelerator currents have increased from 135 and 115 microamperes prior to launch to 185 and 155 microamperes, respectively, in four months. However, the tube charac-

* The output of the diode monitored by channel 92 is positive, so its output is combined with a fixed negative voltage to give a net negative voltage needed by the telemetry circuit.

† The required radiated power at this frequency is only +13 dbm.

TABLE I—CURRENTS, VOLTAGES, POWERS AND TEMPERATURES IN THE ELECTRONICS CANISTER

Channel No.	Function	Universal Time of Telemetry Readings				
		18:11 July 9, 1962	23:03* July 11, 1962	23:15 July 11, 1962	11:51* Nov. 6, 1962	12:03 Nov. 6, 1962
		Readings in bits and units				
1	TWT heater	50 bits	50	50	49	50
		4.7 volts	4.7	4.7	4.75	4.7
3	6390-mc input power	21 bits	11	16	33	11
		−62 dbm	−66.5	−64.5	−60	−66.5
41	IF amplifier temperature	70 bits	64	65	57	59
		86°F	79	81	71	74
4	TWT accelerator	24 bits	24	22	34	32
		115 μa	115	110	163	155
12	TWT collector current	86 bits	85	85	85	85
		17.8 ma	17.6	17.6	17.6	17.6
60	TWT helix current	14 bits	17	16	21	19
		135μa	165	155	200	185
36	Calibration voltage	69 bits	69	70	69	70
		0.23 volt/ bit				
44	277-mc power	102 bits	103	102	104	104
52	255-mc power	109 bits	110	109	112	111
68	Down converter bias 1	43 bits	44	43	43	43
		−4 dbm	−4.1	−4	−4	−4
76	Down converter bias 2	66 bits	66	66	66	66
		−3.9 dbm	−3.9	−3.9	−3.9	−3.9
13	Down converter temperature	74 bits	70	70	64	64
		80°F	77	77	70	70
84	Up converter bias 1	50 bits	55	54	56	55
		17 dbm	+17.45	+17.4	17.45	17.4
92	Up converter bias 2	79 bits	70	70	68	68
		+17.4 dbm	+17.9	+17.9	+17.9	+17.9
29	Up converter temperature	68 bits	64	64	57	57
		82°F	77	77	69	69
99	Reference diode	105 bits	105	105	105	105
		8.4	8.4	8.4	8.4	8.4

* Time when the TWT was turned on. Launch time was 08:35 Universal Time, July 10, 1962.

teristics do not change even when these currents increase to 500 microamperes. The input signals for comparative power measurements must be within the AGC range of −70 to −55 dbm or the 4170-mc drive to the tube will not be the same, and obviously this will cause a change in output at both 4080 and 4170 mc. Since launch there has been almost no change in the 4080-mc output of the tube, so the change in output at 4170 mc from the normal output of 35 dbm has been negligible. The insertion loss of the antenna and feed system is 1.6 db at room temperature, and this loss decreases less than 0.1 db at the low temperatures

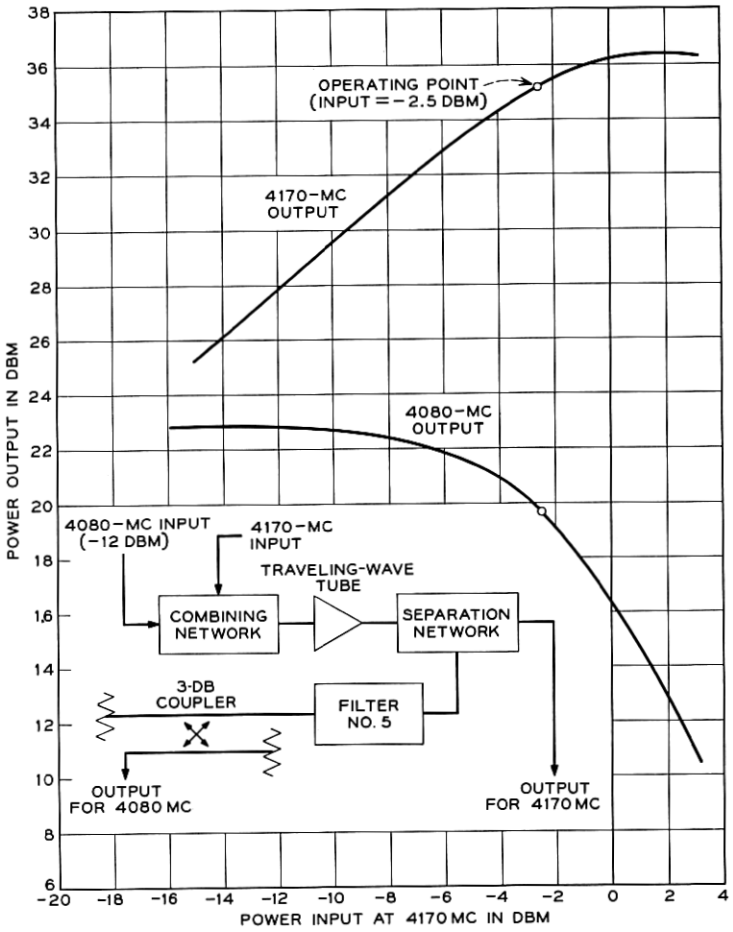

Fig. 18 — Operating characteristics of the traveling-wave amplifier.

encountered in space. At 4170 mc the uncertainty of the antenna insertion loss and the inaccuracies of monitoring 4080 mc by telemetry may give a combined error of ¼ db when calculating the power level, but the radiated power at 4170 mc (33.2 dbm) has not changed appreciably since the satellite was assembled.

8.3 *The Local Oscillator for the Down Converter*

The 6300-mc local oscillator signal for the down converter is obtained from the BO modulator, which combines a signal at 2220 mc from the

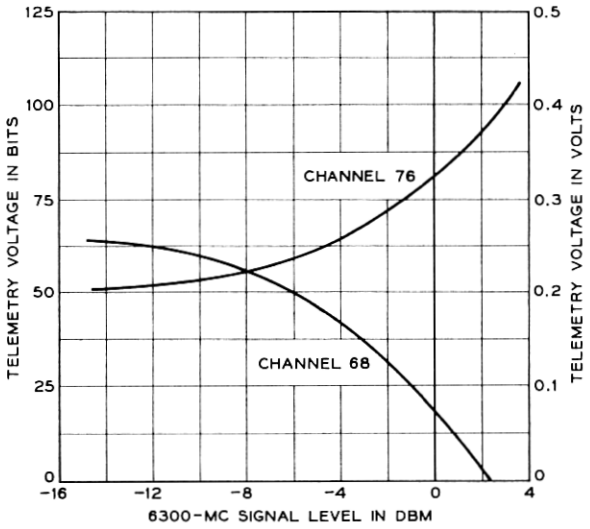

Fig. 19 — Telemetry readings versus local oscillation level for the down converter.

MCS with a portion of the pump signal at 4080 mc. The direct currents in the silicon diodes in the down converter are caused by the RF signal at 6300 mc and by small external dc voltages that forward bias the diodes. Fig. 19 shows the relationship between the telemetry readings of channels 68 and 76 and the level of the local oscillator signal. As is the case with channel 92, used to monitor one of the up-converter currents, the positive output voltage from the down converter is added to an external negative voltage to give a net negative voltage for telemetry. The data in Table I show that the 6300-mc signal has since pre-launch measurements changed only one bit according to channel 68 and no bits according to channel 76. At the operating point, a change of one bit on telemetry corresponds to a change in 6300-mc power level of less than ¼ dbm, so this power has remained almost constant for four months.

8.4 *Power Levels in the Microwave Carrier Supply*

The microwave carrier supply furnishes signals at 2220 and 4080 mc which are used to provide the local oscillator signals for the up and down converters. Each signal is obtained by feeding the output of a crystal oscillator into a transistor frequency multiplier section, which in turn feeds a varactor frequency multiplier section.

8.4.1 *The Transistor Sections*

Each transistor frequency multiplier section in the MCS contains a pseudo AGC system which in all tests prior to installation in the Telstar spacecraft held the VHF power drive to the varactor section constant to within ±0.15 db over a temperature range from 25 to 125°F. The telemetry readings, channels 44 and 52, associated with these powers do not give an accurate measure of power output because changes in transistor characteristics change the calibration. However, if the telemetry reading at a known temperature corresponds to a value taken during bench tests when the power was measured, there is a strong indication that the power is normal. The readings of channels 44 and 52, as shown in Table I, have since launch varied only 3 and 2 bits, respectively. Pre-launch measurements on the completed satellite showed that the readings of these two channels increased with a decrease in temperature. On November 6 the average canister temperature was 7°F below the temperature the day after launch, so the slight increase in the readings of channels 44 and 52 on this date is normal and indicates that the transistor sections of the MCS were normal.

8.4.2 *The Varactor Sections*

The output powers of the varactor multipler sections are not monitored, but these powers can be checked indirectly.

The output power at 2220 mc can be checked indirectly by noting the changes in channels 68 and 76, which measure the level of the power at 6300 mc. A change of 1 db in the 2220-mc signal into the BO modulator, when operating normally, changes the output at 6300 mc by ¾ db, and the BO modulator conversion gain does not change rapidly with temperature. Since the level of the 6300-mc signal has remained essentially constant, the level of the 2220-mc signal could not have changed appreciably.

As is the case with the output of the 2220-mc varactor section, the output of the 4080-mc varactor section is checked indirectly. The 4080-mc power from the MCS is amplified by the TWT and is fed to the pump arm of the up converter. Since any change in the output of the MCS at 4080 mc is translated as an equal change in power to the up converter, channels 84 and 92 indirectly give a measure of the power from the MCS if the tube characteristics and RF power drive are unchanged, as discussed earlier. The measurements made since launch do not show the actual power level of the 4080-mc output of the MCS, but they do show that this power level has not changed appreciably.

8.5 *The VHF Beacon*

Under normal conditions the satellite radiates continuously a 23-dbm signal at 136 mc, used for tracking purposes by the command tracker on the ground. This tracker is completely separate from the tracking equipment associated with the microwave beacon, which is radiated only when the TWT is turned on. When telemetry is turned on, the 136-mc signal is amplitude modulated. This VHF beacon is not monitored by telemetry, so the only check on this power is made by measuring the received ground power and by calculating the transmitted power from known values of path loss and known gains of the satellite and ground antennas. This method is accurate to within ± 1 db when many readings are averaged. Accurate measurements can be made only when the weather is clear and the satellite is above elevation angles of 10°. At low elevation angles, this signal is subject to selective fading.

Measurements of the 136-mc beacon made on the ground prior to launch and in orbit on a weekly basis since launch show that the power has not changed, but day-by-day fluctuations of 1 db, if they existed, could not be detected by these measurements.

IX. CIRCUIT PERFORMANCE CHANGES

In the preceding section, telemetry readings were used to show that power levels of the 255, 277.5, 2220, 4080, 4170, and 6300-mc signals inside the electronics canister had not changed appreciably since launch. Also the method of calculating the transmitted power levels at 136, 4080, and 4170 mc using antenna gains, path loss, and received signal level was discussed. In order to show the invariance of 6300 and 4170-mc signals, it was necessary to show by telemetry that the characteristics of the TWT, MCS, and BO modulator have not changed. In this section, the remaining parts of the satellite circuitry, excluding the radiation experiment circuits, will be discussed from the viewpoint of changes in their operating characteristics.

9.1 *The Down Converter, IF Amplifier, and Up Converter*

In Section 8.2 the methods of checking the output of the tube at 4170 mc were described. The conclusion of this section is that the output power of the TWT, and thus the input power to the TWT at 4170 mc, has remained essentially constant when the input at 6390 mc falls in the AGC range. However, the conversion loss of the down converter, the gain of some stage in the IF amplifier, or the conversion gain of the up

converter could change, and the power drive at 4170 mc to the TWT would remain constant, because the AGC system keeps the power input to the TWT constant by changing the gain of the IF amplifier. If changes occur in the up or down converters or in some part of the IF amplifier, the current through variolossers in the IF amplifier changes to keep the TWT input constant. Channel 3 in the telemetry circuit gives the variolosser current as a function of the input signal to the satellite. Calculations using ground transmitted power, antenna gains, and path loss show that channel 3 readings in space are consistent with readings made before launch. However, the accuracy of this method is no better than 2 db, so the gain of some unit between the input and the TWT could have changed by this amount and it would not have been detected.

9.2 *Nickel-Cadmium Cells*

Since (1) there is no simple way of telling when the Ni-Cd cells are fully charged, (2) the cells may be damaged by excessive discharge and (3) the charging efficiency is a function of state-of-charge, charging current, temperature and past history of the cells, the operating procedure for the Telstar satellite has been very conservative. Graphs are plotted daily showing the state-of-charge of the battery on the basis of a conservative 60 per cent average charging efficiency. Each time the TWT is used, a continuous plot is kept of battery voltage versus time. These plots are compared in an attempt to find changes in the battery, either gradual or otherwise. Two battery discharge curves will be the same only if the battery temperature, the solar-plant current, TWT operate time, and initial battery charge are the same for the two passes compared. The aging of the solar plant due to radiation damage and the variation of eclipse period and its time relative to visibility from Andover, Maine, make exact duplication of conditions for battery comparisons at widely separated intervals impossible. Since these conditions cannot be duplicated, corrections are made in order to get a meaningful comparison. The corrected discharge curves are so similar that they indicate no measurable change in the battery.

9.3 *The Solar Cells*

The solar power plant consists of 50 parallel-connected groups of 72 series-connected silicon n-on-p solar cells covered with sapphire shields 32 mils thick. Fig. 20 shows the average solar plant current from the time the satellite was launched until early January, 1963. These data were taken while the TWT was on, so there is a period of about a month

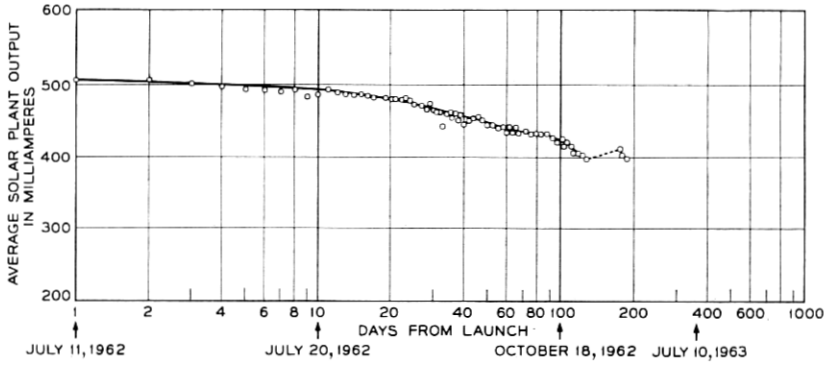

Fig. 20 — Solar plant output.

(December, 1962) when data were not available because of the command malfunction. The points on this graph do not give a perfectly smooth curve because there are, at different times, temperature differences in the solar cells which affect their output. The general shape of the curve shows a degradation due to radiation which by July, 1964, should result in a 32 per cent reduction in capacity.[2]

9.4 *The Voltage Regulator and the dc-to-dc Converter*

The voltage regulator receives power at a varying voltage from the Ni-Cd battery and provides a regulated output of negative 16 volts to power all the transistor circuits and the dc-to-dc converter. When the regulator was first installed in the electronics package, the output voltage of the regulator, as measured by telemetry, remained constant at 96 bits as the load current changed from 0.3 ampere to 1.5 amperes. One telemetry bit corresponds to 0.167 volt. After approximately five months in orbit, the regulated output for all load currents has changed only one bit. It was estimated before launch that radiation damage plus aging might cause the output voltage of the regulator to vary as much as ± 3 per cent, although present data indicate this prediction was pessimistic.

The dc-to-dc converter chops the 16-volt direct voltage from the regulator and steps up the resulting ac voltage with transformers to higher voltages which can be rectified, filtered and applied to the helix, accelerator, and collector electrodes of the TWT. The TWT heater voltage is also obtained by transformer action, but it is only about 4.5 volts. Telemetry is used to monitor the heater voltage and the helix, accelerator, and collector currents for the TWT. Since launch, as Table I

shows, the heater voltage after transients have died out has varied only one bit or 0.08 volt. Increases in accelerator and helix currents shown in Table I result from aging and a slight defocusing of the electron beam in the tube, and are not necessarily caused by increases in voltages. The best proof of the constancy of the TWT voltages is the measure of the output power at 4080 mc, a point discussed earlier. Changes of only 10 volts in the helix voltage (1520 volts is normal) will cause a change of about ½ db in the output of the TWT at 4080 mc. Telemetry readings which monitor this 4080-mc power level indicate a change much less than ¼ db, so the helix voltage has changed very little. The accelerator and collector voltages are derived from the same source as the helix voltage, so they should not have changed either, but there is no direct proof of these voltages remaining constant.

9.5 *Pressure Switches*

The electronics package is hermetically sealed to keep the pressure inside the package at a level of 10 psia. In the event of a leak, the high voltages associated with the TWT would cause corona at critical pressures. One 5-pound and one 1-pound pressure switch (monitored by telemetry) are inside the electronics canister to show the presence of leaks. Since neither pressure switch has operated after six months of operation, even if a small leak exists, no corona problems would exist for several years.

9.6 *The Telemetry System*

While the telemetry does not have a self-check, there are ways to tell something about the unit if some readings are suspicious. The power supply has a reference diode which is monitored by telemetry channel 99, and the telemetry circuit has its own reference diode. Any general error in telemetry readings would show up in channel 99 unless both reference diodes change the same amount. Also, the 16-volt regulated supply is monitored in two places, so differences in these channels could show telemetry troubles. Troubles in the telemetry would probably be first detected by bad readings on many channels. There have been isolated telemetry errors due to external noise pulses in the telemetry receiver on the ground, but in each case an error that occurs in a particular channel on one frame of telemetry information has been corrected on the following frame.

Channels 119 and 120 are used to send out a Barker code[7] and its complement to synchronize the ground telemetry system. It has been

found that when the telemetry is first turned on, the synchronizing signals on channels 119 and 120 are incorrect during the first minute. After one minute, the synchronizing information on these channels is correct.

9.7 *The Command System*

The Telstar command system, as shown in Fig. 16, has redundancy from the diplexer to the relay driver circuits. The output pulse heights of the command receivers are monitored by telemetry channels 86 and 87, and the AGC voltages of the receivers, calibrated to give received RF power levels, are monitored by channels 88 and 89. The receivers can be tested by comparing the output voltages as measured on channels 86 and 87 with similar data taken prior to launch and by comparing the received power levels. The tests on the receiver have been made on a daily basis since launch, and they indicate that there has been no apparent damage to the command receivers.

The T1 and T2 commands are used to test the command receivers and decoders. The T1 command disables decoder 2 for 15 seconds so that command receiver 1 and decoder 1 can be tested; T2 is a similar command which disables decoder 1 for 15 seconds. It was decoder 2 that first gave trouble in the Telstar satellite. This decoder became intermittent on August 8, 1962, became inoperative a few days later, and except for one short intermittent period in mid-October was inoperative until December 21, 1962. On November 23, 1962, after five days of sluggish operation, decoder 1 became inoperative. The cause of the malfunction of the command systems and the measures taken to correct the problem are discussed in a separate paper in this issue.[8]

X. CONCLUSIONS

The launch of the Telstar satellite was highly successful, so the initial orbit, attitude, solar aspect, and spin rate agreed very closely with the predicted values. Most of the data in this report cover the first three months of operation. Subsequent information obtained through January 4, 1963 proves that, except for the command system, the satellite behavior has been normal and predictable. The temperature sensors on the shell show that these temperatures have not exceeded 79°F, which is slightly less than the predicted value. While the electronics equipment operates satisfactorily over a wide temperature range, it is important to see that the average canister temperature has been held at near 70°F throughout the first 1400 orbits. Data from telemetry and from ground

measurements give no indication of any deterioration of the communications repeater or the telemetry system. The command system has obviously been damaged by radiation, but the extent of the present damage after the recovery is not known. The pressure in the electronics canister, as proved by the pressure switches, is at least 5 psi; even if a very small leak does exist, no corona problem associated with the TWT high voltages will exist for several years.

REFERENCES

1. Hatch, R. W., Bennett, S. B., and Kinzer, J. P., Results of the *Telstar* System Communication Tests, B.S.T.J., this issue, p. 1561.
2. Brown, W. L., Buck, T. M., Medford, L., Thomas, E. W., Gummel, H. K., Miller, G. L., and Smits, F. M., The Spacecraft Radiation Experiments, B.S.T.J., this issue, p. 899.
3. Courtney-Pratt, J. S., Hett, J. H., and McLaughlin, J. W., Optical Measurements on *Telstar* Satellite to Determine the Orientation of the Spin Axis and the Spin Rate, to be published.
4. Yu, E. Y., Spin Decay, Spin Precession Damping, and Spin-Axis Drift of the *Telstar* Satellite, to be published.
5. Hrycak, P., Koontz, D. E., Maggs, C., Stafford, J. W., Unger, B. A., and Wittenberg, A. M., Spacecraft Structure and Thermal Design Considerations, B.S.T.J., this issue, p. 973.
6. Davis, C. G., Hutchison, P. T., Witt, F. J., and Maunsell, H. I., The Spacecraft Communications Repeater, B.S.T.J., this issue, p. 831.
7. Chapmann, R. C., Critchlow, G. F., and Mann, H., Command and Telemetry System, B.S.T.J., this issue, p. 1027.
8. Mayo, J. S., Mann, H., Witt, F. J., Peck, D. S., Gummel, H. K., and Brown, W. L., The Command System Malfunction of the *Telstar* Satellite, B.S.T.J., this issue, p. 1631.